DOI 10.24425/aee.2021.136997

Industrial implementations of control algorithms for voltage inverters supplying induction motors

MARIUSZ JABŁOŃSKI, PIOTR BORKOWSKI

Lodz University of Technology
Poland
e-mails: mariusz.jablonski@p.lodz.pl, piotr.borkowski@p.lodz.pl

(Received: 08.11.2020, revised: 11.02.2021)

Abstract: This article discusses the most important issues regarding the implementation of digital algorithms for control and drive technology in industrial machines, especially in open mining machines. The article presents the results of tests in which the algorithm and drive control parameter settings were not selected appropriately for voltage-fed induction motors, and where the control speed was not verified by any of the available motoring or simulation methods. We then show how the results can be improved using field-oriented control algorithms and deep parameters analysis for sensorless field-oriented performance.

Key words: open mining, sensorless control, vector-controlled, adjustable speed drive, converter system, voltage-feed induction motors

1. Introduction to open mining systems

This article discusses problems that occurred in open mining machines when analog control techniques were replaced with digital control systems based on PLC controllers, industrial communication networks, and insulated gate bipolar transistor (IGBT) inverter drive systems. The problems relate to stackers used for handling bulk materials, and were diagnosed either during project commissioning and servicing, or based on scientific observation and technical expertise. They concern the inappropriate choice of algorithms and poor adjustment of the control algorithm to the object, as well as incorrect parameterization of proportional–integral (PI) regulation structures. Changes to motor parameters in transient states in start-up processes and errors related to the identification of the parameters of the equivalent motor model have a great impact on the control stability of the whole drive system. Control problems are dangerous and can cause significant delays in control reactions to setpoint changes, deviations from the operating point,

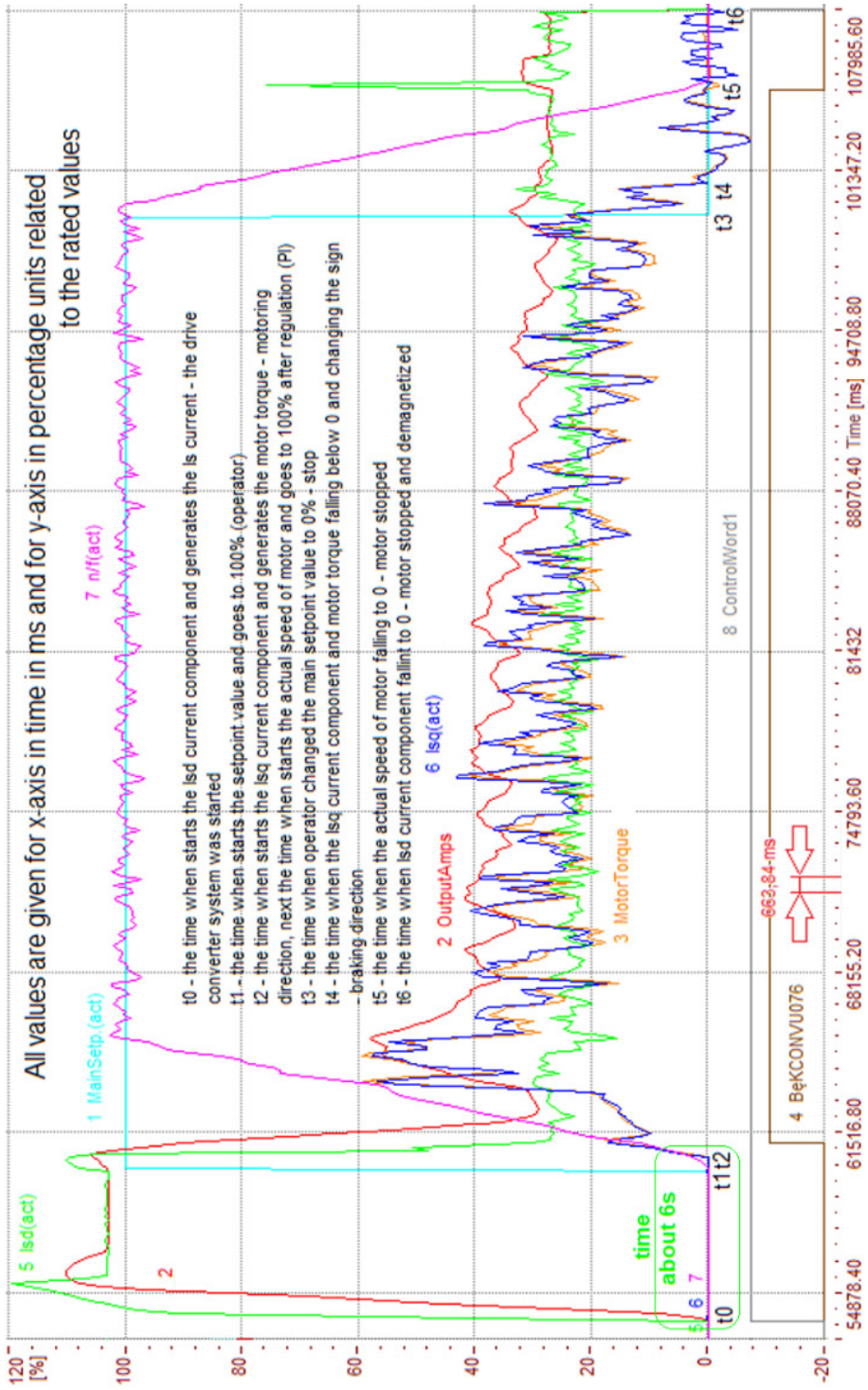

Fig. 1. Start-up process for an induction motor power of 110 KW in a mining stacker ZGOT application with sensorless vector cotrol SVC [3]

unwanted vibrations of the machine construction, as well as to cracks in the subassemblies of large tracked undercarriages and turning mechanisms [1,2]. A number of tests, motion recordings, and analyses were performed on open mining machines, in order to assess the solutions applied in the programming, communication, and drive systems technology [3].

One of the tested machines was a ZGOT 15400.120 stacker. This is the largest type of self-propelled stacker used in opencast mining. The technical and process parameters of the stacker, its scope of work and details of its performance, as well as assessments of its safety, stability, and operational reliability, have been presented in numerous studies e.g. [3, 5, 6]. The drive system of the ZGOT stacker consists of six electromechanical drives with Sgm315M6B type induction motors with nominal power $P_N = 110$ kW for the stacker and two induction motors for the feeder. All of these motors use field-oriented control (FOC) with closed-loop or sensorless vector control (SVC) algorithms for induction motor control. The studied machine suffered from problems during start-up and considerable delays in reacting to control changes. There were also vibrations during normal work. To analyze these problems, the start-up process for the vector-controlled adjustable speed drive with an induction motor (IM) was recorded (Fig. 1).

From the electromechanical waveforms of the ZGOT driving system, with a constant setpoint and SVC control algorithm, it can be seen that during the start-up it first generates the I_{sd} current component. As a result, there are major delays in obtaining the electromagnetic steady state. The time necessary for I_{sd} generation in the case of a motor with 110 kW power and a synchronous speed of 1000 rpm is about 6 s ($t0$ to $t2$). In the inverter parameter settings, it is possible to adjust the generation of the magnetic flux and I_{sd} current component. However, each electrical drive also needs appropriate settings for equivalent motor model parameters and appropriate PI controller settings for speed, torque, and current control. The mechanical system was in good condition, but due to the incorrect settings and errors in the control algorithm it did not function correctly. In Fig. 1, characteristic oscillations in the speed waveforms (curve 7), I_{sq} current component (curve 6), and torque (curve 3) are visible. These are dangerous to the mechanical system and the whole machine [3]. The entire process was divided into time periods (from $t0$ to $t6$), as shown in Fig. 1. After installing the encoders and changing the control algorithm from SVC (open) to FOC (closed), as well as correcting the substitute parameters and selecting the correct settings for the regulators, the machine recovered its ability to make rapid adjustments to the setpoint conditions – see Fig. 7 in [4] and Fig. 8 in [12].

2. Field-oriented closed-loop and sensorless control algorithms

Vector control was patented by Felix Blaschke when he was working for Siemens – U.S. Vector control, Patent 3824437, August 14, 1969 Siemens Germany [10,11]. It is based mainly on a description of induction motor equations [7], which turn an induction motor into a machine very similar to a DC motor. The magnetizing current I_m in a DC machine is by analogy responsible, in an AC machine, for the generation of motor flux (the reactive component I_{sd} of the stator current). The stator current in a DC machine I_a corresponds to the I_{sq} component, represented by the motor torque (active part). Due to the fact that rotor currents cannot be measured directly in squirrel-cage induction motors, they are replaced by equivalent component currents in the selected coordinate system, e.g. d, q, [7]. Then, we have two components of stator current: I_{sd}

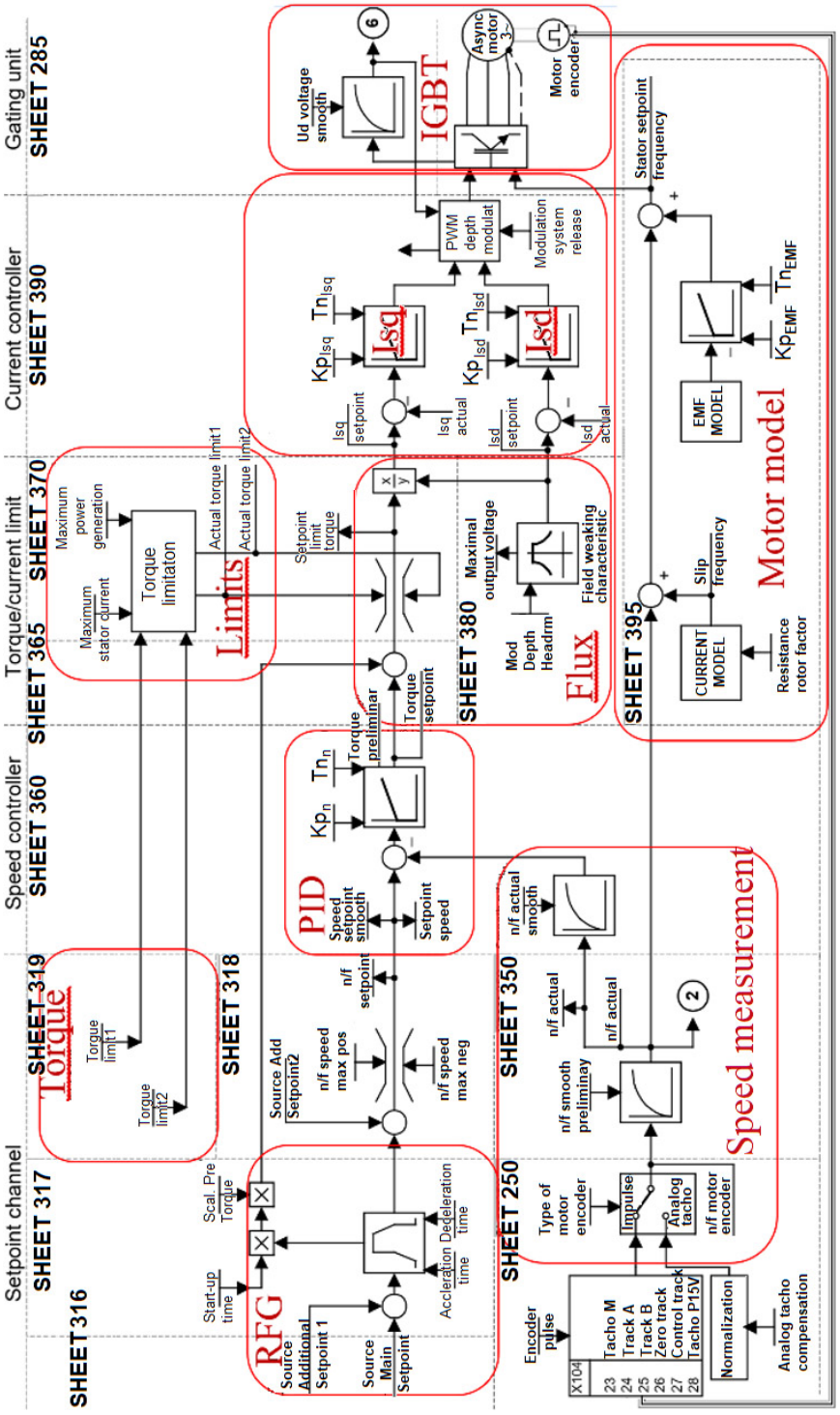

Fig. 2. Vector control algorithm for induction motor controlled by Siemens Simovert MDVC [10, 12]

(flux) and I_{sq} (torque). The conceptions have some weaknesses – i.e., the relationships between the field-oriented components of the stator current I_{sd} and I_{sq}, the output quantities of the frequency converter, as well as between the amplitude of the stator current I_s and the frequency of the stator voltage f_1, do not have strict mathematical equations. The algorithm requires measurements of the phase angles in the machine to synchronize the pulses controlling the frequency of the converter with the course of the rotating flux (Fig. 2).

Fig. 2 presents a block diagram of the vector control algorithm for an adjustable variable speed drive (VFD), the Simovert MasterDrives Vector Control (SMDVC) by Siemens [4,10]. The blocks of the diagram are the basis of the control algorithm used in the vast majority of opencast mining machines with adjustable speed drives in Poland. These devices have very difficult start-up and parameterization processes. Their parameters require very good knowledge of drive techniques and an interdisciplinary approach. On the basis of our research, it can be concluded that numerous applications of these drives in the Polish open mining industry suffer from problems requiring parameter correction [3,4,6].

3. Identification of induction motor parameters for the control algorithm

Identification of the induction motor (IM) equivalent circuit parameters provides information about the connected motor and enables faster responses for the setpoint value by adjusting the speed and torque characteristics. During the parametrization process, basic data from the motor nameplate are used for identification purposes. In the tested device, the maximum current of the stator was set to more than double the nominal current (Fig. 3(a): Motor Rtd Amps $P102$ = 113 A and Imax $P128$ = 230 A – blue frame). The parameters presented in Fig. 3(a), especially resistance and reactance (inductance), are determined by the stator and rotor, magnetizing reactance (inductance) and magnetizing current. As can be seen, the values of the equivalent parameters received from the converter after identification were as follows: R_S = 2.27%; R'_r = 1.28%; $X_s + X'_r$ = 20.92%, X_m = 310.2%; I_m = 28.9% [12]. The motor model is crucial for applying the field-oriented control technique. The induction motor is represented in the drive parameter system as a T model with lumped parameters (Fig. 3(b)) [6].

The model presented in Fig. 3(b) is used as an equivalent motor schema for various operating states and the creation of a phasor diagram of an induction machine. The action is as follows: in the starting state, for setpoint speed $n = 0$ the slip $s = 1$. This means a short-circuit in load. During operation of the model, the current flows in a longitudinal branch through the elements R_S, X_S, X'_r, and R'_r, which allows for determination using the method of current response to a given DC voltage jump. In the no-load state, when speed n rises to n_1 and the slip s falls to 0, the load part approaches infinity. This means there is an open branch in the circuit. After applying voltage, without a load the current will flow mainly through the cross circuit, which allows for the determination of the following parameters: I_m, X_m, and L_m. The R_{Fe} part (not shown in Fig. 3(b)) is very large in relation to the remaining parameters, and is, therefore, ignored. The magnetizing current I_m is the most important parameter for the correct functioning of the chosen vector control algorithms (SVC and FOC). For this reason, in modern adjustable converter drive systems the device manufacturer provides built-in auto procedures for identifying the parameters of induction motors connected to a converter (Fig. 4). Most often, identification is possible when

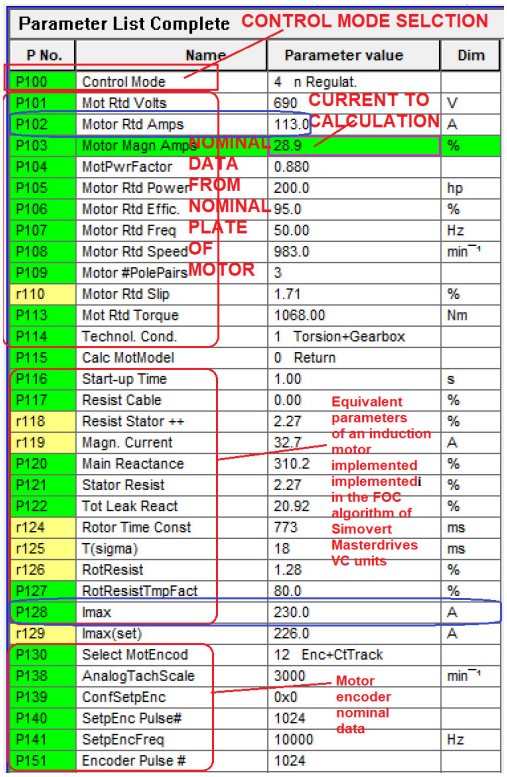

Parameter List Complete — CONTROL MODE SELCTION

P No.	Name	Parameter value	Dim
P100	Control Mode	4 n Regulat.	
P101	Mot Rtd Volts	690	V
P102	Motor Rtd Amps	113.0	A
P103	Motor Magn Amps	28.9	%
P104	MotPwrFactor	0.880	
P105	Motor Rtd Power	200.0	hp
P106	Motor Rtd Effic.	95.0	%
P107	Motor Rtd Freq	50.00	Hz
P108	Motor Rtd Speed	983.0	min⁻¹
P109	Motor #PolePairs	3	
r110	Motor Rtd Slip	1.71	%
P113	Mot Rtd Torque	1068.00	Nm
P114	Technol. Cond.	1 Torsion+Gearbox	
P115	Calc MotModel	0 Return	
P116	Start-up Time	1.00	s
P117	Resist Cable	0.00	%
r118	Resist Stator ++	2.27	%
r119	Magn. Current	32.7	A
P120	Main Reactance	310.2	%
P121	Stator Resist	2.27	%
P122	Tot Leak React	20.92	%
r124	Rotor Time Const	773	ms
r125	T(sigma)	18	ms
r126	RotResist	1.28	%
P127	RotResistTmpFact	80.0	%
P128	Imax	230.0	A
r129	Imax(set)	226.0	A
P130	Select MotEncod	12 Enc+CtTrack	
P138	AnalogTachScale	3000	min⁻¹
P139	ConfSetpEnc	0x0	
P140	SetpEnc Pulse#	1024	
P141	SetpEncFreq	10000	Hz
P151	Encoder Pulse #	1024	

NOMINAL DATA FROM NOMINAL PLATE OF MOTOR

CURRENT TO CALCULATION

Equivalent parameters of an induction motor implemented implementedi in the FOC algorithm of Simovert Masterdrives VC units

Motor encoder nominal data

(a)

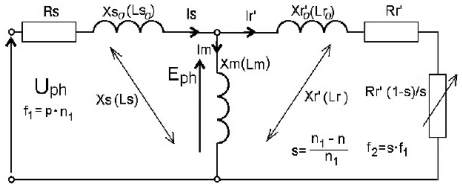

where:
R_S is the resistance of stator windings;
R'_r is the resistance of rotor windings calculated on the stator side;
$X_{S\sigma}$ is the leakage reactance of stator;
X_S is the own reactance of stator windings;
$X'_{r\sigma}$ is the leakage reactance of rotor calculated on the stator side;
X'_r is the own reactance of rotor windings recalculated on the stator side;
X_m is the reactance of magnetization;
I_S is the phase current of stator;
I'_r is the phase current of rotor recalculated on the stator side;
I_m is the current of magnetization;
n is the rotor speed;
n_1 is the synchronous speed;
f_1 is the frequency of stator EMF;
f_2 is the frequency of rotor EMF;
p is the pair of poles;
s is the slip;
U_{ph}, E_{ph} stand for the phase voltage and EMF force.

(b)

Fig. 3. Equivalent parameters of an induction motor implemented in the FOC algorithm of Simovert Masterdrive VC units (a); the T type IM model scheme with equivalent parameters (b) [10, 12]

the shaft is stopped (without disengaging) and when the rotor is moving without a load. The tests are similar to those performed for induction machines: a short circuit test, a no-load test, and a load test. Before starting the procedure, all the necessary parameters for the drive system, motor, and load should be identified, including the machine specifications, the converter, the motor, the mechanics, critical settings, static limitations, and dynamic and control settings [12].

The identification method implemented in the tested drive system belongs to the class of statistical methods. Based on an analysis of the response of the motor to the set DC voltage spike, the parameters of the motor equivalent scheme were determined by comparing the current response waveforms of the test subject to the model. For this purpose, statistical analysis methods were used that iteratively seek such coefficients in the model equations, so that the difference between the waveform obtained from the model and the recorded waveform of the object is zero or negligibly small. During the test, the motor was powered using DC voltage, and therefore did not produce a rotating magnetic field or torque. The drive system was supplied with constant voltage by the symmetrical phase windings of the stator, connected as shown in Fig. 4(a). For

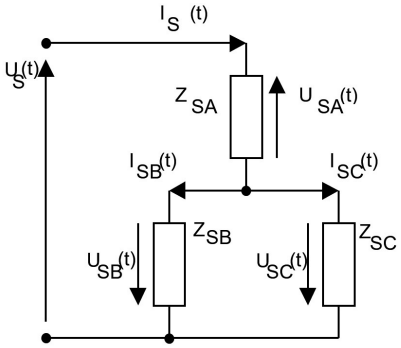

(a)

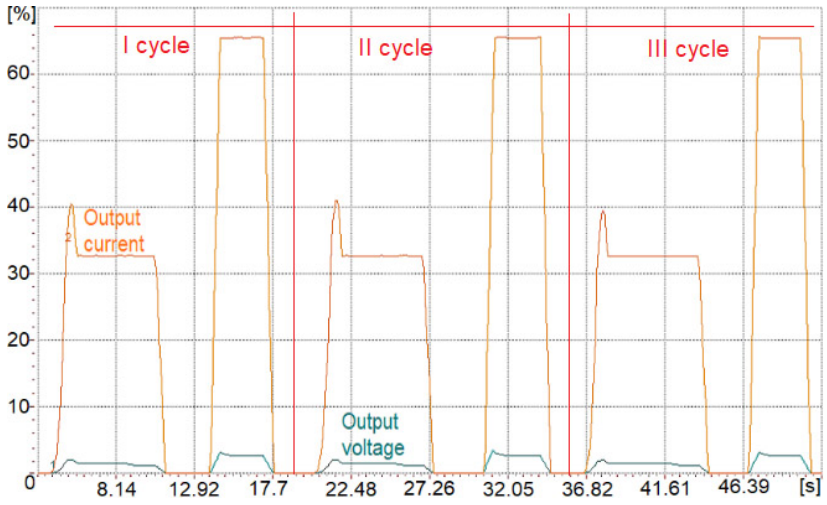

(b)

Fig. 4. Identification of equivalent parameters for an induction motor connected to an inverter in a short-circuit test: connection of the motor phase windings for the short-circuit test (a); identification process for a 55 kW induction motor and Simovert MDVC drive (b). The test takes approx. 55 s [12]

this power supply, the stator U_S supply voltage vector and the stator I_S current vector have only the actual components (U_{sq} and I_{sq} parts). There are therefore no currents or streams in the imaginary axis. This allows us to present the motor model in the form of an equivalent scheme, in which the vector sizes of the current and voltages become scalar values. Since the rotor of the motor remains stationary, the operator transmittance can be determined. The parameters of the equivalent scheme of the motor can be determined by comparing the current response waveforms of the test subject and its model. Determining the equivalent motor parameters may be troublesome, because procedures are realized under difficult environmental conditions and the motor construction is a highly nonlinear object. These parameters, shown in Fig. 3(b) and Fig. 4(a), influence the regulation and operation of the machines [12].

4. Verification of implemented equivalent models of induction motors

An induction motor is a nonlinear, multidimensional object with couplings of controlling signals and internal controlled signals, such as coupled fluxes or electromagnetic torque. The difficulties in controlling such an object can be overcome with the use of spatial vector theory, in a properly chosen coordinate system, describing the dynamics of the induction motor [7]. The Simovert MDVC control system uses two different equivalent models of an induction motor: the current model and the voltage model (EMF – electromotive force) (Fig. 5(a)). The current model acts from 0% to about 10% of the main setpoint value (measurement of the speed is necessary – FOC), or the control system gives the linear function with setpoint current (the sensorless system – SVC). Above this value, the algorithm switches from the current model to the EMF model, without requiring measurement of the rotary speed (Fig. 5(b)). However, errors were observed in the estimation of speed and torque when the equivalent models where switched in both directions (Fig. 5(b)). The final result is a transient state, as the source of oscillations in the waveforms (torque) influences the operating point.

In the current model of the Simovert MDVC (Fig. 5), the speed controller supplies the torque setpoint channel, which is converted into an active current setpoint I_{sq} using an arithmetic circuit. Next, the setpoint torque is converted into a slip setpoint value f_2.

The stator frequency f_1 is calculated by adding the speed and the slip frequency [9]. The current components active I_{sq} and passive I_{sd} (corresponding to I_m magnetizing current) are determined in the current model as actual values from the motor phase currents, relative to the phase position of the motor flux [10]. According to this control concept, a sensor is required to measure the actual speed and the rotor time constant is implemented in the drive parameters. The slip frequency depends on the rotor resistance, but the rotor resistance is not a constant value. It changes together with environmental conditions and the motor temperature. The rotor resistance fluctuates between approximately 60% of its nominal value (cold state) and 100% of its nominal value or above (warm state) [12]. For this reason, the rotor time constant should be corrected to avoid the negative influence of the rotor temperature changes on the slip. The accuracy of the current model can be increased using a temperature measurement sensor [10, 11]. This model is a very good solution if we can provide all the required control signals. Unfortunately, the SVC control algorithm is often used in mining machines, or the closed-loop speed sensor is damaged during FOC operation. This requires the preparation of separate emergency procedures for emergency situations [12].

In the second model, in which the Simovert MDVC control system works with the EMF model (Fig. 5), the drive supplies the motor with the control voltage and the voltage EMF model does not require a tachometer or encoder to measure the actual speed. This is very important for the application of drive systems in opencast mining [4, 6]. The output converter values for currents and voltage are measured and the system should receive the setpoints for the phase angle, by which the voltage leads the flux and the stator current components: I_{sd} active and I_m magnetizing current. Two current controllers, the I_{sq} controller and the I_{sd} controller, ensure that the specified current setpoints are precisely maintained. If the setpoint value of the speed controller changes from 0% to 100% and the active current setpoint I_{sq} also changes from the no-load state to the motor rated-load state, then the actual current is changed to the new actual value (increased). The current phase position is rotated through the value known as the "angle of load" and the

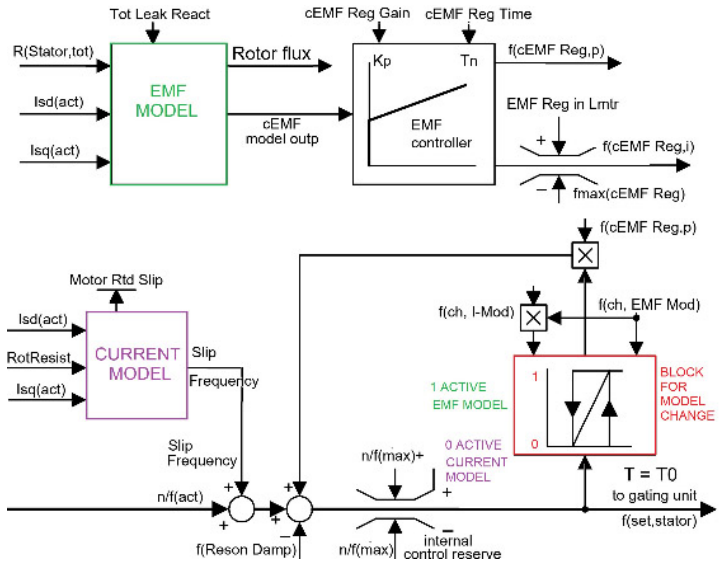

(a)

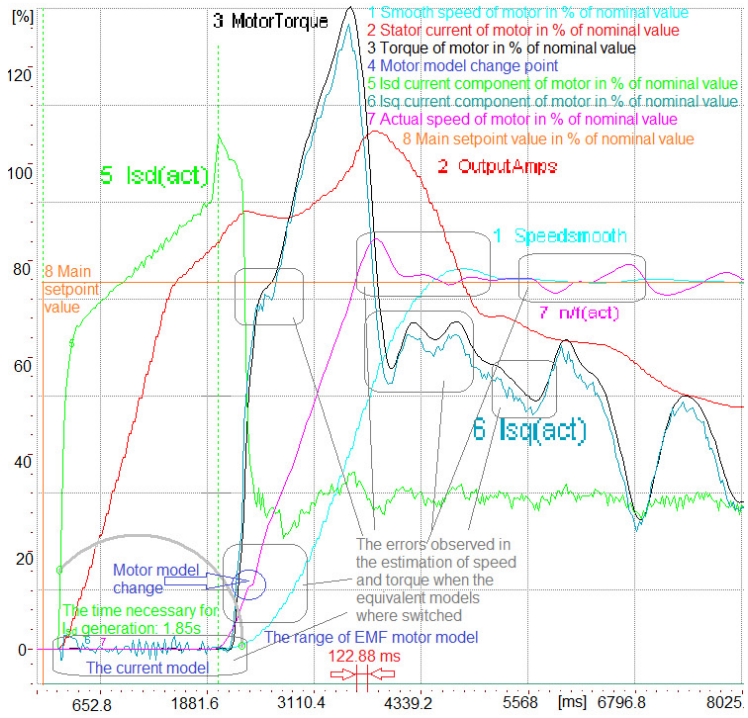

(b)

Fig. 5. Equivalent induction motor models for vector control algorithms FOC and SVC: solution of equivalents models (a); start-up characteristics of ZGOT machine for SVC algorithm (b) [6]

current rotates in accordance with the rotor rotating speed. The new value of the slip frequency f_2 corresponds to the nominal value of the motor torque. The EMF value and the position of the magnetic flux are determined from the actual values (voltage and current) when we analyze the working range of the EMF model. For this reason, the actual value of the motor voltage is required. This value is determined from the gating unit signals and the DC link voltage, but the EMF induced in the motor is calculated in the voltage model from the motor voltage and the measured ohmic and inductive voltage.

In the EMF model, the motor current (flux) and the active stator current components I_{sq} (torque-generating) and I_{sd} (flux-generating) are first obtained. Voltage and frequency are entered so that the actual values for the active current and magnetization current coincide with the appropriate setpoints [10, 11]. However, the EMF model is highly dependent on environmental and motor temperature changes. These changes cause changes in the motor resistance of the stator and the rotor and generally affect the operation point of the machine (especially at low frequencies). Thus, the EMF motor model does not perform well at low speeds and the range around zero frequency is especially problematic for the SVC algorithm [9]. When the frequency f_1 stays at zero, the motor-induced EMF is also zero and there is no EMF value induced in the motor. The position of the magnetic flux cannot be determined. When the machine starts and accelerates from zero to approximately 5–10% (a parameter setting in the hysteresis block – Fig. 5(a)), the speed setpoint value of the control system must be operated in the open-loop controlled mode (Fig. 1 and Fig. 5). During the duty cycle the stacker ZGOT working under changing conditions causes constant changes in the setpoint level, forcing continuous switching between equivalent models (current and EMF, Fig. 5). These continuous changes necessitate constant switching between the current and EMF motor models in both the SVC and FOC vector control algorithms.

The proper selection of an algorithm for the application, parameterization, and verification of motor models is crucial. During the working cycle of the exemplary application for driving a ZGOT stacker, there are continuous changes in the set value level, which force switching between equivalent models. Therefore, this element has a very important impact on the operation of the chosen algorithm, as shown at Fig. 1 and Fig. 5. During the operation of track drives, frequent oscillations occur in the speed, current, and torque of the motor (Fig.6(a)). An insufficiently oversized converter and insufficient motor power can reduce the performance and interrupt the operation of the drive or motor. Broken or cracked mechanical parts are also possible (Fig. 6(b)). The amplitude of oscillations generated in the switching states of the models can be very high, at close to or more than 200% of the nominal motor torque M_N for a setpoint amplitude of about 100% (Fig. 6(a)).

Fig. 6 gives a global overview of the control problem in the starting process of the mining machinery. The resulting situation is undesirable and even dangerous for both the electrical part and the mechanical drive system, with the potential to damage the tracks. Following the analysis, a number of changes were made to the control algorithm, to change the device reaction for setpoint values. The PI regulators settings and equivalent motor model parameters were also corrected. The motor model parameters were calculated and the initial adjustment settings were checked. It is necessary to verify the simulation models before commissioning them, to check the reaction and base rules for the chosen algorithms. Otherwise, insufficient knowledge may lead to a misconception of the nature of phenomena and an underestimation of the maxi-

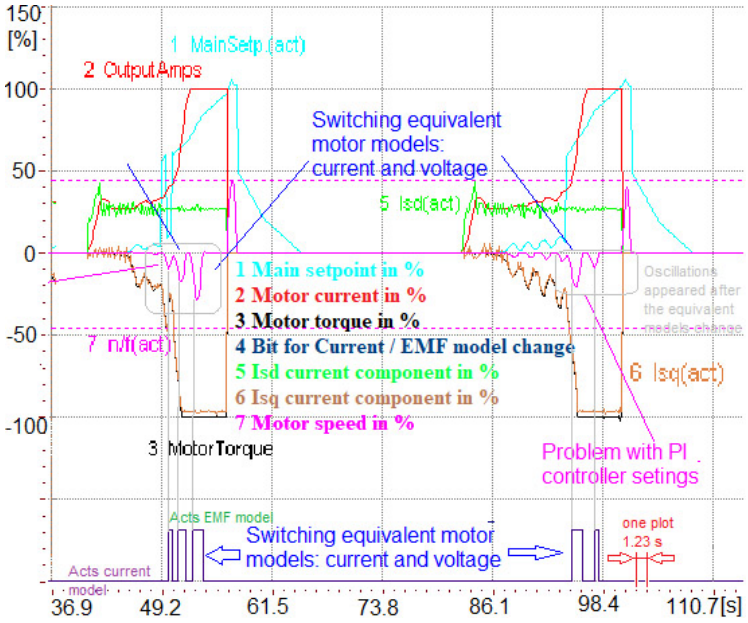

(a)

(b)

(c)

Fig. 6. Example application illustrating FOC operation in the ZGOT stacker: driving for the operating cycle, switching between EMF and current model (a); cracked subassemblies of the large-size tracked undercarriage of a caterpillar chain (b) and balance lever units (c) [1, 2, 12]

mum settings and electromechanical calculations, as well as to a lack of information about the interactions of the designed control algorithms. The risks may be difficult to predict. Firstly, service and maintenance are at risk and dangerous. Secondly, in many machines, cracks may appear in the tracks. Running repairs are possible, but cracks in the construction structure may also unfortunately cause a complete breakdown of the machine and require lengthy and costly renovation [1, 2, 12].

5. Electromagnetic transitional processes in electrical inverter drives

For industrial applications with electrical drives, changes in the working states (starts, braking, load change, set value changes) are an inevitable feature of their operation. However, it is important, since it has a decisive influence on the operation of the system and in ensuring the required dynamics, to adjust the required quantities (current, speed, torque, flux) the first few times the drive is switched on. The starting process with a description of the individual stages is shown in Fig. 7, including the start signal, generation of the I_{sd} component, generation of the I_{sq} component, and starting on the ramp. The process of establishing the electromagnetic state of the motor takes about 1.5–2 s (this is the time counted from the "start" signal to speed $n > 0$). After the start signal, only the stator current I_{sd} component appears (curve 5), whereas the stator current I_{sq} component (curve 6) appears after a delay. The value of the I_{sd} component begins at the level set based on the value of the magnetizing current (steady excitation, determined by the parameter setting). In the first range of operation, a very small voltage is applied to the motor terminals and this induces the appropriate flux. Next, motor torque (curve 3) appears and the motor starts ($t3$).

The analysis of the functioning the FOC algorithm in a closed-loop system with a given speed feedback signal shows that it is possible to reduce the delay time that occurs when the motor starts. This is possible by adjusting the settings of the parameters leading to a time reduction in the block responsible for generation of the I_{sd} current component (excitation time). In addition, when using FOC algorithms in situations in which we want to minimize the delay time during start-up, the control should use both components of the stator current I_{sd}, I_{sq} independently. The torque is adjusted by changing the component I_{sq} and stator current, to which we have direct access. The course of the accident stator current (curve 2) of both components and its effective, according to the equation:

$$I_s = \sqrt{I_{sd}^2 + I_{sq}^2}\,.$$

The current I_s is compared with the constant value of the parameter determining the maximum current of the motor and must meet the condition

$$I_s = \sqrt{I_{sd}^2 + I_{sq}^2} \leq I_{s\,\max}\,.$$

As a result, when the stator current is insufficient the difference is that the stop element does not transmit the signal $I_{s\,\max} - I_s > 0$ and the current limitation system does not respond. In this case, the slip pulsation ω_r can be calculated by taking into account both components d and q,

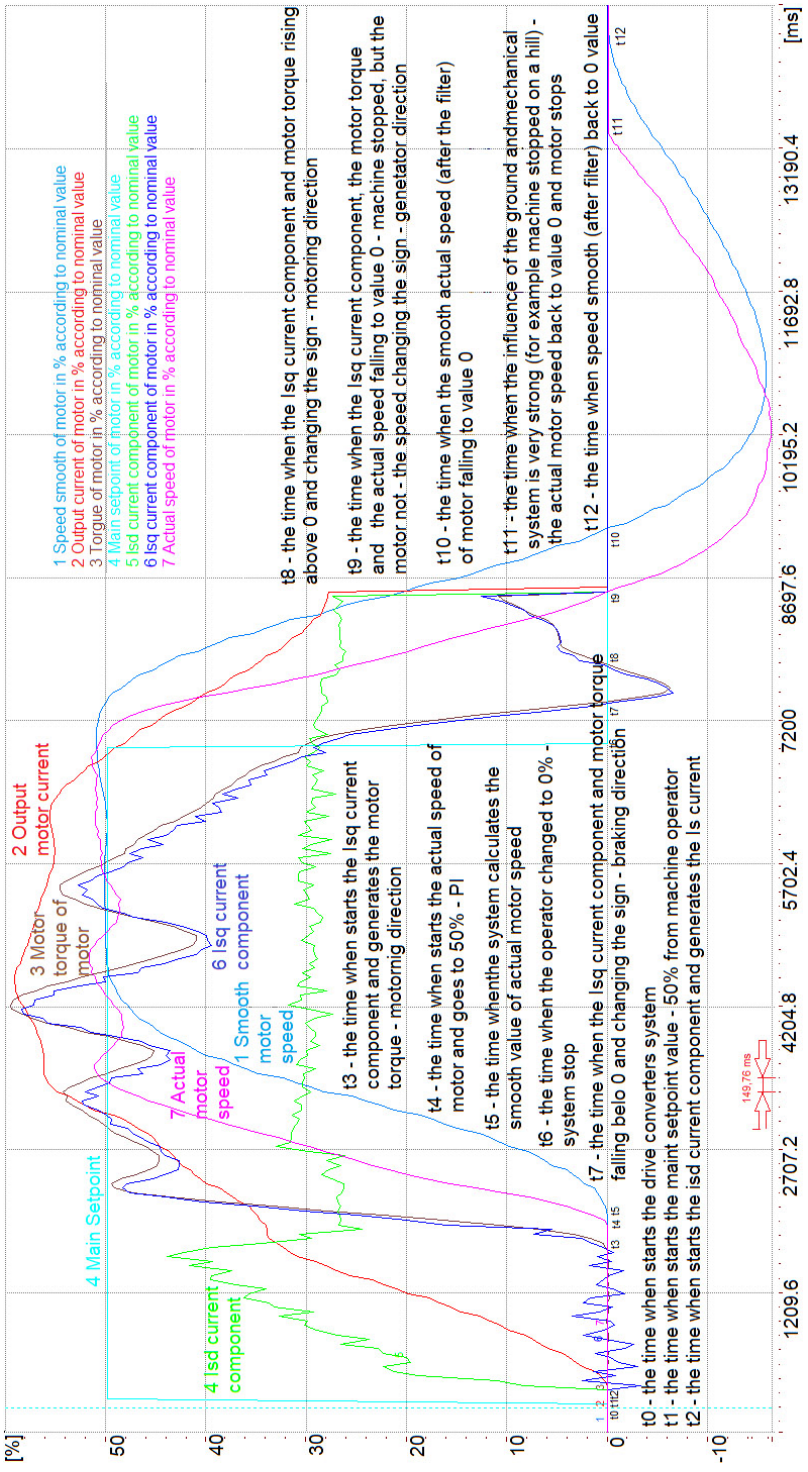

Fig. 7. Schedule of changes in total active power at the input of the load node

according to [9]:

$$\left.\begin{aligned} &\frac{\mathrm{d}\Psi_r(t)}{\mathrm{d}t} = \frac{\mathrm{d}\Psi_{rd}(t)}{\mathrm{d}t} = -\frac{\Psi_{rd}(t)}{T_r} + \frac{i_{sd}(t)\cdot L_m}{T_r} \\ &M(t) = \frac{3}{2}\cdot p \cdot \frac{L_m}{L_r}\cdot\left[\Psi_{rd}(t)\cdot i_{sq}(t)\right] \end{aligned}\right\} \Rightarrow \omega_r = \frac{i_{sq}(t)\cdot L_m}{T_r\cdot\Psi_{rd}(t)} \quad \text{and} \quad T_r = \frac{L_r}{R_r}, \tag{1}$$

where: T_r is the time constant of the rotor and I_s is the motor current of the stator.

System equations describing the rotor of the induction motor tested in the component system d, q, are given in [7]. A vector state equation for a cage induction machine, takes into account the overlap of the d-axis with the stream vector and assumes that the component Ψ_r is zero [8].

Under fixed conditions, in the steady state, the current component I_{sd} is constant. The magnetizing current I_m representing the rotor stream and the component of the stator current I_{sq}, representing the torque of the motor, also have constant values. The relationship between the stator current components I_{sd} and I_m is as follows [9]:

$$I_{sd} = I_m + T_r\frac{\mathrm{d}I_m}{\mathrm{d}t}\,. \tag{2}$$

Note that in all cases there is significant over-regulation of the stator current for the component I_{sd}. The reason is the inertia with which Ψ_{rd} appears in the rotor axis as a response to current

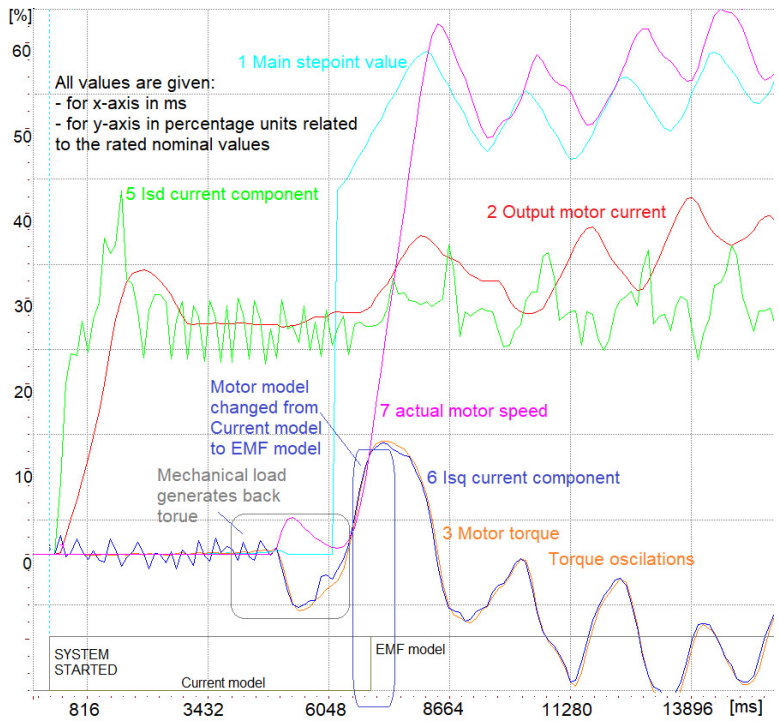

Fig. 8. Start-up forward run characteristics for the F2U11 loading elevator (feeder) before modification of the control algorithm [12]

extortion. It is desirable that the value of the flux, and thus the value of the component I_{sd}, is determined by the time of the appearance of the component I_{sq} stator current. This allows the electromagnetic torque of the motor to be adjusted by controlling only the component I_{sq}. The existing overregulation in the component run I_{sd} allows the stream value to be set at the required level (pre-defined). The equation binding the component I_{sd} of the stator current to the rotor Ψ_{rd} in the axis d is as follows [9]:

$$\frac{\mathrm{d}\Psi_{rd}}{\mathrm{d}t} + \frac{R_r}{L_r} \cdot \Psi_{rd} = \frac{L_m \cdot R_r}{L_r} \cdot I_{sd} \,. \tag{3}$$

I_{sd} (flux) is generated by pre-set characteristics and the four-quarter characteristics $M = f(n)$ of the motor should be taken into account Fig. 8. The set point in the system has the magnetic fluctuation of the motor from the beginning. Correct identification of the parameters of the motor equivalent scheme is crucial for the proper functioning of the model and the drive.

6. Modification of control algorithm parameters

Experimental investigations of ZGOT work were executed for different parameters of the motor and control system (Fig. 9). The modifications enabled a substantial reduction in oscillations

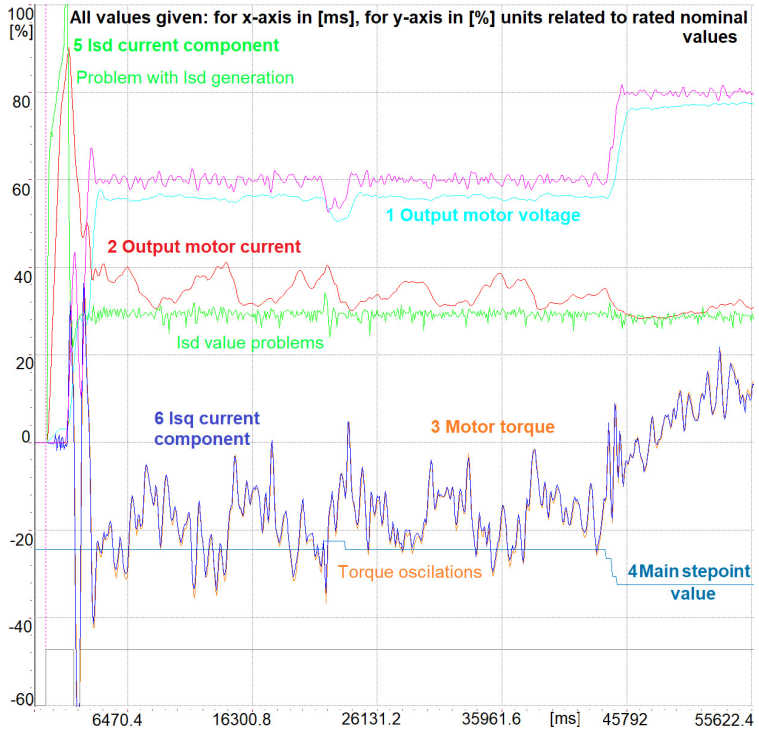

Fig. 9. Curves showing characteristic quantities during startup and forward runs of the loading elevator (feeder) and F2U11 caterpillar after modification of control algorithm [6, 12]

in the torque, speed, and current of the motor during a forward run of both caterpillars of the loading elevator F2 (feeder).

The maximum values of the current did not exceed 100% of the current limit. Thus, they were considerably lower than the values obtained with the standard control algorithm. The modifications also made it possible to eliminate the frequent faults caused by exceeding the over-current limits. The effectiveness of the proposed modifications was confirmed both under laboratory and industrial conditions.

7. Conclusions

This article has presented the results of tests on the algorithm and drive control parameter settings of voltage-fed induction motors. We have shown how these results can be improved by using field-oriented control algorithms and in-depth analysis of parameters for sensorless field-oriented performance. Current calculations of the equivalent parameters of motors at different temperatures can be used as the basis for the implementation of the adaptation function in response to changes in the rotor winding equivalent resistance depending on temperature changes. Improvement of the control properties, especially under difficult operating conditions, can be achieved by taking into account changes in the rotor resistance under the influence of temperature in the calculations of the motor parameters. For the correct implementation of the selected FOC or SVC algorithm, determining the value of the magnetizing current is a key issue. The parameter settings that reflect the engine model and the basic characteristics of the powertrain are also of primary importance. Long delays in the feedback loops may cause temporary loss of stability in the control systems of mining machines. It is therefore advisable to check the construction of loops and adjustments. Carrying out periodic inspections of machines using inverter drive technology can help to identify control problems more rapidly.

References

[1] Kaczyński P., Czmochowski J., *Analysis of causes for cracks in the connection of the swivel drawbar with crawler beam of the feeder vehicle*, Mechanical Faculty, Wrocław University of Technology, Mining and Geoengineering, Book 2, no. 33, pp. 169–177 (2009).

[2] Sokolski P., Sokolski M., *Evaluation of resistance to catastrophic failures of large-size caterpillar chain links of open-pit mining machinery*, Eksploatacja i Niezawodność – Maintenance and Reliability 2014, vol. 16, no. 1, pp. 80–84 (2014).

[3] Anuszczyk J., Jabłoński M., *Modification of the sensorless algorithm for controlling the drives of the tracks of the ZGOT Roller*, Mining Institute of the Wrocław University of Technology, no. 112, pp. 69–76 (2005).

[4] Anuszczyk J., Jabłoński M., *Research of electromechanical power units of the ZGOT*, International Congress of Surface Mining, Bełchatów (2009).

[5] Kanczewski P., Kowalczyk P., *ZGOT-15400.120 first Polish 200,000*, Scientific work of the Mining Institute PWr. III International Congress of Lignite Mining, Bełchatów, pp. 213–221 (2002).

[6] Jabłoński M., Borkowski P., *Replacement of control systems with implementation of digital inverter drive technology in surface mining machines*, Conference KOMTECH 2020, to be published.

[7] Paszek W., *Dynamic of alternating current electrical machines*, Helion, Gliwice (1998).

[8] Pełczewski W., Krynke M., *Variable State Method in Drive System Analysis*, WNT, Warszawa (1984).

[9] Tunia H., Kaźmierkowski M., *Automation of converter dries systems*, PWN, Warszawa (1987).

[10] *Technical documentation, engineering manual and compendium for SIMOVERT MASTERDRIVES*, Automation and Drives, Variable-Speed Drive Systems, Erlangen 1999-2012, Siemens AG (2020).

[11] *Technical documentation, engineering manual and compendium for SINAMICS drives*, Automation and Drives, Variable-Speed Drive Systems, Erlangen 1999-2012, Siemens AG (2020).

[12] Jabłoński M., *Analysis of functional parameters and modification of control algorithms of field-oriented inverter drive with induction motor*, PhD., Faculty of Electrical Engineering, Electronics, Computer Science and Automation PŁ, Łódź (2006).